REACTANT AND CATALYST STRUCTURE/FUNCTION RELATIONSHIPS IN HYDROCRACKING OF BIPHENYL MOIETIES

Carole J. Read, Stephan Schwarz, and Michael T. Klein
Center for Catalytic Science and Technology
Department of Chemical Engineering, University of Delaware
Newark, Delaware 19716

Keywords: hydrocracking, biphenyl, CoMo-Y-Zeolite

1.0 INTRODUCTION

Catalytic hydrocracking is a flexible refining process that can accommodate a wide range of feedstocks and generate a range of useful products. Part of this flexibility derives from the use of a bifunctional catalyst. A metal function allows for hydrogenation of polynuclear aromatics (PNA's) and dehydrogenation of alkanes to olefin intermediates. An acid function promotes isomerization and cracking. Acting in concert, these functions and the process conditions of temperature, hydrogen pressure, WHSV, etc., combine to lower the molecular weight and increase the H/C ratio of the feedstock.

Clearly the feedstock specifications also play a crucial role. For example, in PNA hydrocracking, the apparently subtle reactant structural feature of six versus five carbon-containing rings can lead to important process implications. The hydrocracking of PNA's containing exclusively six-carbon-membered rings, such as anthracene, phenanthrene and naphthalene, proceeds by the predominant patterns [1-3] of: terminal ring hydrogenation, followed by cyclohexyl ring isomerization, ring opening and dealkylation to yield a lower molecular weight aromatic product and light gases (e.g., C_4). On the other hand, the reaction of the five-carbon-membered ring containing PNA fluoranthene (I) involves hydrogenation to tetrahydrofluoranthrene, center ring opening to 5-phenyl tetralin, and biphenyl bond cleavage to tetralin and benzene, as shown in Equation 1.[4]

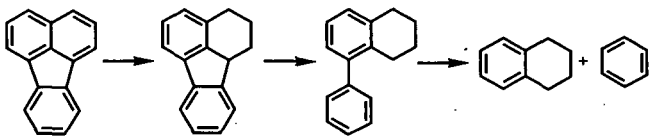

(1)

Table 1 summarizes important hydrocracking pathways of fluoranthene[4], 9-ethyl fluorene, 9-phenyl anthracene, and 2-phenyl naphthalene deduced from reactions with H_2 and an industrial equilibrated NiMo/USY-Zeolite catalyst. These model compounds all generate structures that can undergo the direct biphenyl cleavage. Inspection of Table 1 reveals the minimum structural moiety for direct biphenyl cleavage. Fluoranthene, 2-phenyl naphthalene, and 9-phenyl anthracene, all fully aromatic, require hydrogenation and cracking steps before they have the structure capable of direct biphenyl cleavage which occurs from rows III to IV in Table 1. In contrast, 9-ethyl fluorene has aliphatic character and as a result requires fewer transformations before forming 2-propyl biphenyl, which can be directly cleaved.

It is also instructive to consider the reactions of related compounds that did not follow the efficient bond cleavage pathway. Fluorene, for example, ring opens to 1-phenyl toluene, which contains a benzylic hydride but not the additional β saturated carbon whose deprotonation to an olefin would allow hydrogenation to afford the final alkyl-substituted product [5]. 2-Methyl biphenyl likewise suffers from the same structural deficiency, and undergoes only isomerization reactions. Biphenyl does not directly cleave to form two moles of benzene per mole of biphenyl reacted; rather, it is postulated that cracking occurs via cyclohexyl benzene. Thus the *minimum structure necessary for efficient cleavage is proposed to be a biphenyl moiety with an alkyl group,*

comprising at least two carbons, bonded ortho to the biphenyl bond.

Additional experiments with the NiMo/USY-Z industrial catalyst and 9-ethyl fluorene revealed kinetically significant reactions: cleavage of the center fused cyclopentyl ring, transalkylation, and condensation reactions to form 9-methyl phenanthrene. Comparison of the 5-phenyl tetralin and 2-propyl biphenyl intermediates observed from reaction of fluoranthene and 9-ethyl fluorene, respectively, highlights the causes of these new pathways. The formal [1,5] shift is the only significant pathway for 5-phenyl tetralin. In contrast, the n-propyl group can participate in ring closure and transalkylation. Thus somewhat subtle changes in reactant structure can engender a wide range of available pathways. It is reasonable to expect similar sensitivity with regard to catalyst structure.

The reactions noted above comprise several key molecular transitions: hydrogenation, the net [1,5] biphenyl cleavage, center ring opening of cyclopentyl ring, isomerization, transalkylation, and ring closure. Each of these is influenced by the catalyst properties to a different degree. Herein, we report the preliminary work aimed to determine the catalyst function that influences the kinetics of each.

As a first step, the acidity of the catalyst was probed by varying the sodium content of the zeolite-Y support. The procedure used followed the early work of Ward [6-9] and Hansford and Ward [10,11]. These workers concluded that the concentration of Bronsted acid sites increases linearly with decreasing sodium content of the zeolite until 60-70% of the sodium ions have been replaced. They also found that o-xylene isomerization activity increased with decreasing sodium content. The activity per site also increased with decreasing sodium content.

The foregoing suggests that hydrocracking reactivity can be viewed as a rate functional,[12] which combines structure/function relations f(S) for both the catalyst (S_C) and reactant (S_R). Observed reactivity $\boldsymbol{R}$ is thus a function of both $f(S_C)$ and $f(S_R)$, as in Equation (2).

$$\boldsymbol{R} = R\ \{\ f(S_C),\ f(S_R)\ \} \qquad (2)$$

The objective of this paper is to report the results of hydrocracking experiments with a standard commercial catalyst and a range of reactant molecules, as a probe of $f(S_R)$, and also experiments involving a probe reactant (9-ethyl fluorene) and a range of carefully prepared catalytic materials that mimic aspects of the industrial catalyst. The goal is to lay a foundation for unraveling more quantitative aspects of $\boldsymbol{R}$.

2.0 EXPERIMENTAL PROCEDURES

2.1 Material Synthesis

The catalysts prepared for the present work were designed as follows: both commercial (Strem Na-Y zeolite) and synthesized zeolite were used. Sodium zeolite Y was synthesized following an early patent by Breck [13]. Zeolite-Y was synthesized from an aged gel and then washed and filtered. The samples were dried overnight at 110°C and then calcined under a flow of air. The calcination program was heating at 350°C for three hours and then calcining at 500°C for four hours.

A series of acid supports was made by ion exchanging either commercial or synthesized zeolite-Y with ammonium nitrate solutions. The hydrogenation activity was provided by sulfided CoMo. The metal loading and introduction methods are as reported by Cid and co-workers [14-16]. The metal function was varied through the use incipient wetness impregnation, ion exchange/impregnation, and rotary vacuum impregnation.

2.1 Zeolite Characterization by XRD and TEM

X-Ray powder diffraction (XRD) of the zeolite samples was accomplished using a Philips XRG 3000 x-ray generator coupled to an APD 3520 controller. The radiation employed was CuKa with a wavelength of 1.540562 A. All samples were scanned from 6° to 60° 2Θ. The peak heights above the background of the 5

largest peaks of calcined NaY were used to compute % crystallinity according to:

$$\% \text{ Crystallinity} = \frac{(\Sigma \text{hts. of 5 peaks})\text{sample}}{(\Sigma \text{hts. of 5 peaks})\text{standard}} \times 100$$

Metal oxide and metal sulfide species in the catalyst samples were identified using Table 2 which lists the characteristic peaks for each of the non-zeolitic phases.

Transmission electron microscopy (TEM) of the samples was accomplished using a Philips EM 400 transmission electron microscope. The sample was prepared for microscopy by dispersing some of the zeolite in n-hexane, transferring a drop of the suspension onto a copper grid and allowing the solvent to evaporate. The average crystal size of the parent zeolite, n, was obtained from micrographs by counting and measuring ~ 200 crystals. Note that $n = \Sigma(d_i n_i)/\Sigma n_i$ where d_i is the diameter of the ith particle and n_i is the number of crystals of diameter i.

2.2 Catalytic Hydrocracking Reactions

The hydrocracking pathways and kinetics of 9-ethyl fluorene, 9-phenyl anthracene and 2-phenyl naphthalene in the presence of an equilibrated NiMo/Z-USY were studied at 310-380°C and 153 atm hydrogen. Experimental methods are detailed elsewhere [4,17]. In brief, hydrocracking experiments were conducted in a batch autoclave or in batch agitated tubing bombs. Experiments conducted in the stirred batch autoclave were in the presence of hexadecane solvent, whereas reactions in the tubing bombs were without.

Additionally, the hydrocracking of 9-ethyl fluorene, 1-phenyl naphthalene, biphenyl, and naphthalene in the presence of the synthesized catalytic materials were studied at 325°C and 153 atm. hydrogen pressure. These experiments were conducted in 12-cm^3 SS agitated tubing bombs in the absence of solvent.

For all types of experiments, the catalyst was ground to 80-100 mesh. It was then sulfided with 90% H_2/10% H_2S at flow rate of 30 cm^3/min for 2 hours at 400°C. Gas chromatography and gas chromatography/mass spectrometry were used to identify liquid-phase reaction products.

3.0 RESULTS AND DISCUSSION

3.1 Zeolite Characterization

XRD analyses showed that $CoMoO_4$ was found in all samples whether the cobalt be introduced by impregnation or ion exchange. Co(imp)Mo(imp)NaY also showed evidence of Co_3O_4, but after exchange with NH_4^+ and subsequent calcination, this oxide could no longer be detected. MoO_3 could not be unambiguously assigned to any of the samples, except for Co(imp)Mo(imp)NaY, since its two strongest lines very nearly coincide with NaY lines [15]. The sulfided Co(ex)Mo(imp)NaY did not contain x-ray crystalline Co_9S_8 or MoS_2. Note, however, that since the detection limit of XRD is ~ 2nm, the above results do not necessarily imply that the oxide and sulfide species mentioned were absent.

Table 3 lists the crystallinities of the calcined materials. Clearly impregnation decreased crystallinity. This has also been reported by Cid et al. [14,15] who observed crystallinities < 40% for high Mo loadings (9% and above). The loss of crystallinity upon impregnation was ascribed to the partial destruction and distortion of the zeolite lattice by the interaction of molybdate anions with framework oxygen. It was noteworthy that impregnation by the rotary evaporation technique yielded slightly more crystalline materials than the incipient wetness technique. When Co was incorporated into the zeolite by aqueous ion exchange prior to Mo impregnation, the reduction in crystallinity was far less pronounced.

The results from the TEM showed an average crystal size of 0.7 μm, with a size range of 0.2 - 1.1 μm.

3.2 Reactant and Catalyst Structure/Function

Preliminary reactions are reported with the following materials: a CoMo impregnated Strem sodium zeolite-Y (Co(I)Mo(I)/Na-Y), Co ion exchanged Mo impregnated Strem sodium zeolite-Y (Co(ex)Mo(I)/Na-Y), and a CoMo impregnated onto a twice ammonium exchanged, calcined Strem sodium zeolite-Y (Co(I)Mo(I)/Strem 2X ex NaH-Y). All impregnations used the incipient wetness technique. Reactions with biphenyl, naphthalene, 9-ethyl fluorene, and 1-phenyl naphthalene reactants revealed broad trends. Under the reaction conditions of 325°C, 150 atm hydrogen, the main reaction product yield and selectivities are summarized in Table 4.

The first catalyst used was the Co(I)Mo(I)/Na-Y. Naphthalene,1-phenyl naphthalene, 9-ethyl fluorene, and biphenyl were separately contacted. For naphthalene and 1-phenyl naphthalene, the main reaction was hydrogenation. Naphthalene hydrogenated to tetralin; no decalins were observed. The selectivity to tetralin formation was 54% after 30 minutes reaction time. The naphthalene moiety of 1-phenyl naphthalene was preferentially hydrogenated as the main product was 1-phenyl-1,2,3,4-tetrahydronaphthalene. The hydrogenation kinetics of naphthalene and 1-phenyl naphthalene were of the same order of magnitude. Biphenyl and 9-ethyl fluorene did not react over this catalyst.

The second catalyst examined was a Co(ex)Mo(I)/Strem Na-Y. Naphthalene, 1-phenyl naphthalene, 9-ethyl fluorene, and biphenyl were individually reacted.

Naphthalene hydrogenated to tetralin with the cobalt exchanged catalyst; some transalkylation reactions occured to form methyl naphthalenes. The selectivities for tetralin, 2-methyl naphthalene, and 1-methyl naphthalene were 59, 7.4, and 4.2%, respectively, after 25 minutes reaction time. The kinetics of hydrogenation were of the same order of magnitude as with the previous catalyst sample.

1-Phenyl naphthalene preferentially reacted to form 2-phenyl naphthalene (selectivity of 69%, 30 minutes). All four hydrogenation products of 1-phenyl and 2-phenyl naphthalene also formed. The temporal variation of products' yields showed that 1-phenyl and 2-phenyl-1,2,3,4 tetrahydronaphthalenes cleaved to form tetralin and benzene.

Biphenyl underwent predominantly transalkylation reactions to form methyl biphenyls and fluorene with the Co(ex)Mo(I)/Na-Y catalyst. No single ring cleavage products were observed.

Finally, 9-ethyl fluorene was exposed to the Co(ex)Mo(I)/Na-Y catalyst. The center cyclopentyl ring cleaved to form 2-propyl biphenyl (selectivity of 0.75%). No single ring aromatics or naphthenics were observed in the product spectrum. The intermediate 2-propyl biphenyl did undergo ring closure to form 9-methyl-9,10-dihydrophenanthrene and, ultimately, 9-methyl phenanthrene (selectivity of 1.8, 3.8%, respectively, 32 minutes). Transalkylation reactions were dominant, forming methyl,ethyl-fluorenes with a selectivity of 45%, 32 minutes.

The third catalyst was a Co(I)Mo(I)/2x(ex) NaH-Y. The reaction of 9-ethyl fluorene led to center ring cleavage and transalkylation as the predominant reactions. The selectivity to 2-propyl biphenyl was 2.6% (40 minutes). The selectivity for the transalkylation products was 11% after 40 minutes.

Acknowledgement:

We gratefully acknowledge the support of this work by Sun Refining and Marketing Company. Additional acknowledgements are to Mr. Ralph Bertolacini and Dr. Simon Kukes of Amoco Oil and Dr. James Lyons and Mr. Aris Macris of Sun Refining and Marketing Company.

References:

(1) Lemberton, J.; Guisnet, M. *Applied Catalysis* **1984**, *13*, 181-192.
(2) Martens, J. A.; Jacobs, P. A.; Weitcamp, J. *Appl. Catal.* **1986**, *20*, 283 - 303.

(3) Haynes, H. W. J.; Parcher, J. F.; Helmer, N. E. *Ind. Eng. Chem. Proc. Des. Dev.* **1983**, *22*, 401 - 409.
(4) Lapinas, A. T.; Klein, M. T.; Gates, B. C.; Macris, A.; Lyons, J. E. *Ind. Eng. Chem. Res.* **1987**, *26*, 1026 - 1033.
(5) Lapinas, A. T.; Klein, M. T.; Gates, B. C.; Macris, A.; Lyons, J. E. *Ind. Eng. Chem Res.* **1991**, *30*, 42 - 50.
(6) Ward, J. W. *Journal of Catalysis* **1967**, *9*, 225-236.
(7) Ward, J. W. *Journal of Catalysis* **1967**, *9*, 396-402.
(8) Ward, J. W. *Journal of Catalysis* **1968**, *10*, 34-46.
(9) Ward, J. W. *Journal of Catalysis* **1968**, *11*, 251-258.
(10) Ward, J. W. and Hansford, R. C. *Journal of Catalysis* **1969**, *13*, 316-320.
(11) Ward, J. W. and Hansford, R. C. *Journal of Catalysis* **1969**, *13*, 364-372.
(12) Astarita, G. *Thermodynamics: An Advanced Textbook for Chemical Engineers*; Plenum Press: New York, 1989, pp pp.93-96.
(13) Breck, D. W. In *Crystalline Zeolite Y*; 1964; U. S. Patent No. 3,130,007
(14) Cid, R.; F. Orellana *Applied Catalysis* **1987**, *32*, 327-336.
(15) Cid, R., F. J. Gil Llambias, J. L. G. Fierro, A. L. Agudo and J. Villasenor *Journal of Catalysis* **1984**, *89*, 478-488.
(16) Cid, R., J. Villasenor, F. Orellana, J. L. G. Fierro, and A. L. Agudo *Applied Catalysis* **1985**, *18*, 357-372.
(17) Lapinas, A. T. PhD Thesis, University of Delaware, 1989.

Table 1. Chemical Moieties Susceptible to Efficient Biphenyl Cleavage

Row	Fluoranthene	9-Ethyl Fluorene	9-Phenyl Anthracene	2-Phenyl Naphthalene
I	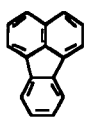		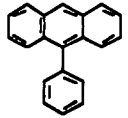	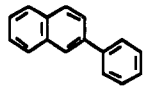
II	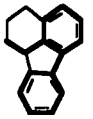	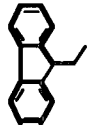	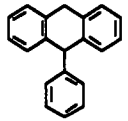	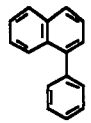
III	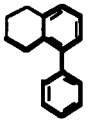	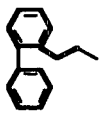	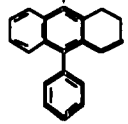	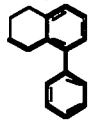
IV	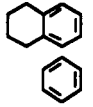	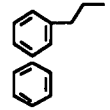	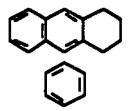	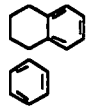

Table 2: Identification of non-zeolitic phases

Species	Largest peak (2Θ)	2nd largest peak (2Θ)
Co_3O_4	36.8°	31.3° (*)
MoO_3	27.3° (*)	23.3° (*)
$CoMoO_4$	26.5°	23.3° (*)
Co_9S_8	52.0°	29.9° (*)
MoS_2	14.4°	39.5° (*)

(*) : partial overlap with NaY peaks

Table 3: XRD Crystallinities of metal-zeolite Y materials

Catalyst	% Crystallinity
NaY	100
NaHY(2x exch.)	100
Co(imp)Mo(imp)NaY	25
Co(imp)Mo(imp)NaHY(2x exch.)	30
Co(imp)Mo(imp) rot. vap. NaY	45
Co(imp)Mo(imp) rot. vap. NaHY (1x exch.)	40
Co(ex)Mo(imp)NaY	90
Co(ex)Mo(imp)NaY, sulfided	70

Note: rot. vap. = impregnation by rotary evaporation. Other samples impregnated by incipient wetness

Table 4. Hydrocracking reaction selectivities for naphthalene, 1-phenyl naphthalene, 9-ethyl fluorene, and biphenyl

Reactant:	Naph	1-PN	Naph	1-PN	9-et fl	biphenyl	9-et fl
catalyst:	1	1	2	2	2	2	3
T, °C	325	325	325	325	325	325	325
P/atm (at T)	150	150	150	150	150	150	150
t, min	30	21	25	30	32	25	40
conversion of reactant	0.057	0.065	0.634	0.877	0.111	0.035	0.075
Product Selectivities							
benzene				6.71E-02		3.55E-02	
cyclohexyl benzene						2.84E-02	
methyl indans			3.11E-03				
tetralin	5.42E-01	2.79E-02	5.90E-01	7.14E-02			
naphthalene		1.89E-02		8.69E-03			
methyl tetralins			2.82E-02	1.16E-03			
2me naphthalene	1.60E-02		7.39E-02	6.01E-04			
1me naphthalene	5.46E-02		4.18E-02	5.04E-04			
2-methyl biphenyl						3.70E-02	
3-methyl biphenyl						1.35E-01	
4-methyl biphenyl						4.15E-01	
hexahydro fluorenes					2.46E-02		1.37E-01
2propyl biphenyl					7.54E-03		2.59E-02
mw 168's					1.21E-01		1.38E-01
hexahydro-9et-fluorenes					3.54E-02		1.89E-01
fluorene, 38.09					5.94E-03	1.20E-01	6.52E-02
9-me dihydro phenanthrene					1.78E-02		
methyl 9-et fluorenes					4.54E-01		1.10E-01
ethyl 9et fluorene, 53.18					4.50E-02		6.75E-02
9-me phenanthrene, 60.4					3.75E-02		5.99E-03
1-phenyl tetralin		3.51E-01		1.04E-02			
5-phenyl tetralin		9.74E-02		6.97E-03			
2-phenyl naphthalene				6.90E-01			
phenyl tetralins				1.88E-01			
methyl phenyl naphthalenes				1.02E-02			

1 = Co(I)Mo(I)/Na-Y
2 = Co(E)Mo(I)/Na-Y
3 = Co(I)Mo(I)/2XNaH-Y